Switch Voltage Rating Selection Considering Cost-Oriented Redundancy and Modularity-based Trade-offs in Modular Multilevel Converter

Ahmadi, Miad; Shekhar, Aditya; Bauer, Pavol

DOI
10.1109/TPWRD.2023.3263270

Publication date
2023

Document Version
Final published version

Published in
IEEE Transactions on Power Delivery

Switch Voltage Rating Selection Considering Cost-Oriented Redundancy and Modularity-Based Trade-Offs in Modular Multilevel Converter

Miad Ahmadi, *Graduate Student Member, IEEE*, Aditya Shekhar, *Member, IEEE*, and Pavol Bauer, *Senior Member, IEEE*

***Abstract*—Modular Multilevel Converters (MMCs) find increasing applications in medium to high-voltage systems. In such systems, reliability-oriented selection of power electronic switches becomes essential because higher modularity implies an increased number of components. The trade-off between the impact of higher modularity on converter reliability is quantitatively established, corresponding to redundancy costs for the given lifetime requirements. Therefore, this paper proposes a method for an optimal choice among available market switch voltage rating for the MMC. It is shown that the sub-modules (SMs) based on 1.7 kV switches are the most suitable (instead of 1.2 kV and 3.3 kV switches) for two case studies adapting data from the medium voltage grid in The Netherlands. Moreover, the insights from these case studies are generalized to DC link voltage in the range of 10–220 kV and average loading of 1–100%. The sensitivity analysis is performed for the different failure rates (FRs), required lifetime, components cost, and energy price. Sensitivity analysis is also performed to identify the impact of FIDES and Military Handbook (MIL-HDBK) methods. The impact of converter power capacity is studied under the variable current rating. Finally, a generalized form of the proposed method is presented and applied in the published works.**

***Index Terms*—Modular multilevel converter (MMC), redundancy, modularity, reliability analysis, cost assessment, sensitivity analysis.**

I. Introduction

GRID-CONNECTED power electronics converter are getting more attention due to climate change, renewable energy sources integration, and fossil-free transportation [1]. The extensive interconnection of power electronics-based systems into power grids is affecting the reliability of the system. Modular multilevel converter (MMC) is an attractive topology among others for medium to high voltage applications [2]. MMC is a promising candidate due to its modularity, scalability, high efficiency, and superior harmonic performance [3]. However, higher modularity consequently increases the number of components in the system, thereby influencing the risk of failure [4]. Therefore, the cost-effective design for reliability by considering the trade-off between modularity and redundancy is important [5].

For the MMC design, reliability and cost-based methods by only considering redundancy are reported in [6], [7], [8], [9]. In [6], the cost-based model of the MMC with two redundancy strategies is evaluated, and it is presented that standby redundancy has a lower cost than active redundancy. Authors in [7] present an optimization method by considering the cost and redundancy aspects of the MMC with hybrid sub-modules (SMs). In [8], a method is proposed that provides reliability indices to plan periodic preventive maintenance for the MMC in off-shore applications. In [9], three converter topologies, including 2-level, 3-level neutral-point-clamped (NPC) and MMC with fixed switch voltage rating of 4.5 kV are compared for Medium Voltage (MV) applications. Analysis of [9] shows that using 3-level NPC is the most economical when the rated current is below 400 A and DC link voltage is below 56 kV. If the rated current is in the range of 500 A-700 A and DC link voltage is above 46 kV, MMC is the most cost-efficient choice. Likewise, for the current rated above 700 A, regardless of DC link voltage, MMC is the most cost-efficient converter. The design of the MMC that only focuses on redundancy are well-explored in [10], [11], [12], [13], [14], where the system reliability is improved by applying different redundancy strategies. For instance, in [11], a redundancy strategy is proposed where the redundant SMs can be shared among all arms. It is presented that with this redundancy strategy, the number of required redundant SM is decreased by 33% compared to the conventional redundancy strategies.

Modularity (switch voltage rating) is another factor in the MMC that can play an important role in the reliability and cost (initial investment and operational loss) aspects. Few works [15], [16], [17], [18] have reported on the design of the MMC by considering modularity aspects of the MMC. In [15], a mission profile method is proposed to design the 17 MW 28 kV DC link MMC with the focus on modularity to suggest that SM with switches of 3.3 kV voltage rating are the most reliable and cost-efficient choice as compared to other market available ratings. The impact of redundancy is considered in [16], and

Manuscript received 17 October 2022; revised 24 January 2023 and 28 February 2023; accepted 25 March 2023. Date of publication 30 March 2023; date of current version 25 July 2023. Paper no. TPWRD-01547-2022. *(Corresponding author: Miad Ahmadi.)*

The authors are with the Electrical Sustainable Energy, Delft University of Technology, 2628 CD Delft, The Netherlands (e-mail: m.ahmadi-3@tudelft.nl; a.shekhar@tudelft.nl; p.bauer@tudelft.nl).

Color versions of one or more figures in this article are available at https://doi.org/10.1109/TPWRD.2023.3263270.

Digital Object Identifier 10.1109/TPWRD.2023.3263270

TABLE I
COMPARISON OF THE EXISTING LITERATURE AND PROPOSED STUDY FOR MMC DESIGN

Reference	Mod†	Red‡	Cost	Varying DC link vol	Varying loading
[15]	✓		✓		✓
[16]	✓	✓		✓	
[9]		✓	✓	✓	✓
[18]	✓	✓	✓		
[6]–[8]		✓	✓		
[10]–[14]		✓			
Current study	✓	✓	✓	✓	✓

† Modularity ‡ Redundancy

it is suggested that 3.3 kV switch is the optimal choice for line-to-line AC side voltages between 22 kV and 58 kV in an MV cascaded H-bridge AC-DC converter. In [17], the reliability of the MMC by applying individual insulated-gate bipolar transistor (IGBT) SM using Hipak style IGBTs, and series valve SM using press-pack IGBT are compared. It is shown that using Hipak style IGBTs has the lowest conduction losses, while for the first few operational years, presspack IGBTs are more effective in preventing the arm's voltage from decreasing, and the need for installing redundant SMs decreases. [18] compares the semiconductor with different rated voltages to find the optimum choice based on SM utilization and losses for high-voltage direct current (HVDC) applications. Authors conclude that HVDC in the power range below 900 MW, 4.5 kV switch is optimal. For the power range between 900 and 1000 MW, both switches with rating voltage of 4.5 kV and 6.5 kV have similar performance, while the switch with rating voltage of 6.5 kV is optimal for power range above 1000 MW.

Table I summarizes and compares the existing literature with the proposed method in this study. In the current paper, both concepts of redundancy and modularity as two aspects of reliability in the MMC are combined to suggest the optimum voltage rating of the switch. Concerning costs, the insights of [15] are extended by considering the costs associated with redundancy and its corresponding sensitivity to different system parameters such as DC link voltage, average converter loading, required lifetime, and energy price. This paper aims to quantitatively establish the trade-off between the impact of higher modularity on converter reliability corresponding to the redundancy costs for the given lifetime requirements while considering the operational efficiency. The key contributions of this study are as follows:

- Quantify the MMC's trade-off between modularity and redundancy by varying the submodule switch rating and suggesting the optimal number of levels for the given DC link voltage and operating power with consideration of the capital cost, efficiency, and reliability aspects.
- Derive a generalized insight on selecting the optimal switch rating considering the above trade-off with varying DC link voltage, power rating, average loading, required lifetime, failure rate (FR), components cost and energy price.
- It also investigates the influence of using two different methodologies (Military Handbook (MIL-HDBK) and FIDES) for calculating the FR of components and the effect of various current ratings.

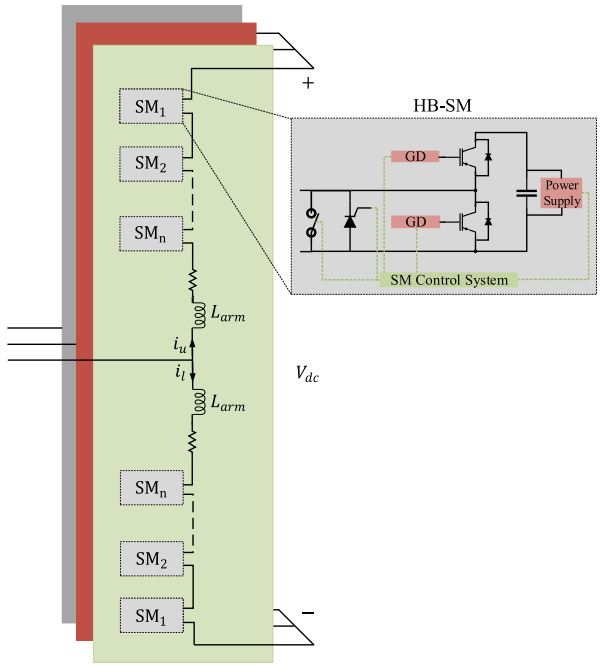

Fig. 1. Illustration of an MMC with half bridge sub-modules.

The rest of the paper is organized as follows. In section II, the characteristics of the system and the method for analyzing the MMC reliability are given. Section III defines a case study and evaluates the system's cost, reliability, and efficiency. Sensitivity analysis is carried out in section IV. In section V, the general application proposed in this paper is recommended, and the paper is concluded in section VI.

II. System Description and Reliability Design

This section provides a system description and the methodology for evaluating the reliability.

A. Modularity Design

The general configuration of the MMC with half-bridge (HB) SM is presented in Fig. 1. MMC is composed of three phases, and each phase has two arms. Each arm has a number of SMs connected in series with arm inductance. In this study, as an example, the considered MMC system has rated power (S_n) of 10 MVA with line voltage (V_g) of 8.16 kV. The DC link voltage (V_{dc}) can be estimated by [16]:

$$V_{dc} = \frac{2\sqrt{2} \times V_s}{\sqrt{3} \times m} \tag{1}$$

where m is the modulation index and it is equal to 0.96, V_s is the RMS of line to line voltage equal to $\sqrt{3}/\sqrt{2}\ V_g$. The minimum number of required SMs (N_{min}) in each arm depends on the selected power switch rating. Besides this, the maximum value of SM capacitors voltage ripple k_{max} needs to be considered (which in this study is equal to 10%). Hence, N_{min} is defined as

TABLE II
MMC PARAMETERS FOR FIVE DIFFERENT SWITCHES RATING

V_{IGBT} (kV)	V_{dc} (kV)	N_{min}	f_{sw} (Hz)	C_{SM} (mF)	$V_{SM,av}$ (kV)	$S_{f,act}$
	(1)	(2)		(3)	(4)	(5)
1.2	17	24	125	9.2	0.71	0.650
1.7	17	17	177	6.5	1.00	0.647
3.3	17	9	334	3.4	1.89	0.629
4.5	17	7	429	2.7	2.43	0.594
6.5	17	5	600	1.9	3.40	0.575

(2) [19]:

$$N_{\text{min}} = \text{Ceil}\left[\frac{k_{\text{max}} \times V_{\text{dc}}}{S_{\text{f}} \times V_{\text{IGBT}}}\right] \tag{2}$$

where Ceil (x) function returns the smallest integer that is greater than or equal to x, S_{f} is the safety factor of IGBT that can be determined based on the voltage limits for steady-state operation of MMC, V_{IGBT} is the IGBT blocking voltage. In this paper, the safety factor is equal to 0.65, which is in the range of maximum steady state voltage of IGBT [18]. A design element that plays a crucial role in the cost, reliability, and operation of MMC is the SM capacitor. The time-average stored energy and peak value of capacitor voltage are needed to determine the SM's capacitor. According to [19], the required capacitor is given by:

$$C_{\text{SM}} = \frac{N_{\text{min}} \times S_{\text{n}} \times W_{\text{MMC}}}{3(k_{\text{max}} V_{\text{dc}})^2} \tag{3}$$

where W_{MMC} is the required energy storage per MVA that is approximately 40 kJ/MVA as defined in [20].

The operating switching frequency (f_{sw}) is chosen in this study such that the effective frequency ($f_{\text{eff}} = N_{\text{min}} \times f_{\text{sw}} \approx$ 3 kHz) is constant for the chosen switch rating with the given DC link voltage. This ensures that the harmonic performance of the designed converter is compliant with IEEE 519 with similar power quality for the same arm/filter inductance when different switch ratings and hence the number of levels are selected [21]. Correspondingly, the varying switching and conduction losses for different operating frequencies and the number of levels can be calculated while ensuring that harmonic performance is the same for the given DC link voltage. Table II summarizes the number of SMs per arm, SM capacitance, and switching frequency which are all defined based on the withstand voltage of the IGBT module (V_{IGBT}).

Herein, N_{min} is given by (2) and the average operating SM voltage ($V_{\text{SM,ave}}$) is given by (4).

$$V_{\text{SM,ave}} = \frac{V_{\text{dc}}}{N_{\text{min}}} \tag{4}$$

Consequently, the actual operating safety factor ($S_{\text{f,act}}$) associated with maximum SM voltage is given by (5),

$$S_{\text{f,act}} = \frac{k_{\text{max}} V_{\text{SM,ave}}}{V_{\text{IGBT}}} \tag{5}$$

As observed, $S_{\text{f,act}}$ is closer to the initial design value S_{f} for lower switch rating due to the impact of ceiling function in (2). Consequently, it results in a slightly lower switch utilization and SM FR with higher switch ratings. This effect is reduced when a second ceiling function is applied with redundancy requirements for the given B_{10} lifetime, as discussed in the subsequent section. Furthermore, difference in switch utilization in trade-off with reliability is further reduced for higher DC link voltages as shown in Fig. 2.

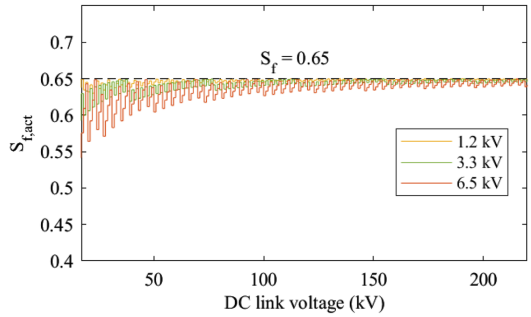

Fig. 2. The actual safety factor value with varying DC link voltage.

B. Reliability Design

For reliability analysis of MMC, the FR of the components within the MMC needs to be evaluated. Also, redundancy as a fault-tolerant strategy is applied to increase the MMC reliability [22]. The following scrutinizes the FR of power components and the redundancy effect.

1) FR Calculation: In MMC, SMs construct the arms, and its configuration is shown in Fig. 1. The SM is composed of two IGBTs, a capacitor bank, and auxiliary components [10]. The FR of the switches and capacitor can be calculated by using equations from the MIL-HDBK [23] as (6) and (9).

$$\lambda_{\text{MIL-IGBT}} = \lambda_{\text{base-IGBT}} \pi_{\text{T}} \pi_{\text{S}} \pi_{\text{A}} \pi_{\text{R}} \pi_{\text{E}} \tag{6}$$

where $\lambda_{\text{base-IGBT}}$ is the base FR of IGBT equals to 100 FIT [6]; π_{T} is the temperature factor calculated as (7); π_{S} is the factor for voltage stress formulated as (8); π_{A} stands for the application factor; π_{R} defines the power rating factor, and π_{E} is the environmental factor [6].

$$\pi_{\text{T}} = exp\left[-2114 \times \left[\frac{1}{T_{\text{j}} + 273} - \frac{1}{298}\right]\right] \tag{7}$$

$$\pi_{\text{S}} = 0.045 \times exp\left[3.1 \frac{V_{\text{applied}}}{V_{\text{rated}}}\right] \tag{8}$$

where T_{j} is the junction temperature, V_{applied} and V_{rated} are the actual and nominal voltage across the IGBT, respectively.

$$\lambda_{\text{MIL-Cap}} = \lambda_{\text{base-Cap}} \pi_{\text{T}} \pi_{\text{V}} \pi_{\text{SR}} \pi_{\text{Q}} \pi_{\text{E}} \pi_{\text{C}} \tag{9}$$

where $\lambda_{\text{base-Cap}}$ is the base FR for film capacitor that is equal to 100 FIT [6]; π_{SR} defines the influencing factor of the series resistance of the capacitor; π_{Q} is the quality coefficient; π_{E} stands for environmental factor; π_{C} is the capacitance coefficient, π_{V} is the voltage stress factor calculated as (10), and π_T is the temperature factor formulated as (11) [6].

$$\pi_V = \left[\frac{V_{\text{operating}}}{0.6 \times V_{\text{rated}}}\right]^5 + 1 \tag{10}$$

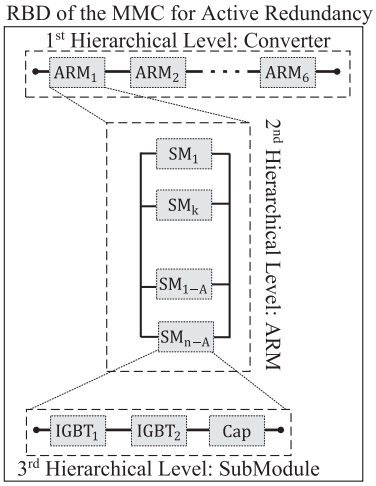

Fig. 3. RBD model of MMC under active redundancy.

$$\pi_T = exp\left[\frac{-0.15}{8.617\times10^{-5}}\left[\frac{1}{T_j+273}-\frac{1}{298}\right]\right] \tag{11}$$

where T_j is the ambient temperature, which depends on the loading of the converter. In this study, it is assumed if the MMC is not operating (0% loading), the junction temperature of the capacitor and IGBT is equal to the ambient temperature (25° C) and If it operates at full load (100% loading), the junction temperature is 100° C. So, the junction temperature can be estimated at any chosen loading. $V_{\text{operating}}$ and V_{rated} are the actual and nominal voltage across the capacitor, respectively.

2) Redundancy Evaluation: Redundancy as a fault-tolerant strategy is applied to have a normal post-fault operation without degradation [24]. Different redundancy strategies are explored in [10], [20] and the optimal choice depends on many factors such as efficiency, dynamics, economics. This article applies the fixed-level active redundancy strategy [6], [9], [16], and the reliability block diagram (RBD) of MMC with this redundancy is presented in Fig. 3. In this redundancy strategy, the number of operating SMs within the arm always equals N_{min}. However, in this operating mode, all the SMs (n) are energized, but the triggering signal is only sent to random N_{min} SMs. Hence, all the SMs take turns operating. In this redundancy strategy, triggered SMs could be either original or redundant [16]. As it is shown in Fig. 3, in fixed-level active redundancy operational state, if $N_{\text{red}} = \text{n-}N_{\text{min}}$ is the number of redundant SMs in each arm, the reliability of the arm can be calculated by applying k-out-of-n given by (12) [25].

$$R_{\text{arm}}(t) = \sum_{N_{\text{min}}}^{n} C_n^{N_{\text{min}}} R(t)^{N_{\text{min}}} (1-R(t))^{n-N_{\text{min}}} \tag{12}$$

$$R(t) = e^{-\lambda_{\text{SM}} t} \tag{13}$$

$$\lambda_{\text{SM}} = 2\times\lambda_{\text{MIL-IGBT}} + \lambda_{\text{MIL-Cap}} \tag{14}$$

where λ_{SM} is failure of the SM with N_{min} operational SM. For calculating the MMC reliability, since there are six arms, the MMC's reliability is formulated as (15)

$$R_{\text{MMC}}(t) = (R_{\text{arm}}(t))^6. \tag{15}$$

3) Reliability Index: In this study, the percentage of the lifetime B_α is used, which determines what percentage of devices fail at the time as (16):

$$F_{\text{MMC}}(B_\alpha) = 1 - R_{\text{MMC}}(B_\alpha) = \frac{\alpha}{100} \tag{16}$$

where unreliability function F_{MMC} represents the proportion of population failure. B_{10} lifetime is expressed as the required time to reach 90% of the system's reliability (or 10% of devices fails). Hence, the number of redundant SMs is selected in the design process to reach the required B_{10} lifetime. Table III shows the B_{10} lifetime of the MMC without redundancy and having one redundant SM in each arm with different switch ratings (obtained from Fig 4(a) and (b) respectively).

TABLE III
OBTAINED B_{10} LIFETIME IN YEARS (FIG. 4(A) AND (B)) FOR 10 MW 17 KV DC LINK MMC WITH DIFFERENT SWITCH RATINGS

Switch ratings		1.2 kV	1.7 kV	3.3 kV	4.5 kV	6.5 kV
B_{10} lifetime	No red	0.12	0.17	0.34	0.48	0.72
	One red	1.31	1.85	3.63	5.14	7.44

According to [6], [9], [26], [27], the required lifetime of power electronic systems can vary from 2 years to more than 30 years. Still, the necessary lifetime in most applications falls between 5 to 20 years. Hence, this paper considers B_{10} lifetime of 10 years as the reliability index for determining the number of redundant SMs in each arm. Additionally, the sensitivity analysis will be carried out in the case if the required B_{10} lifetime is 5 and 20 years.

Fig. 4(a) and (b) show the reliability of the MMC with different switch voltage ratings at 57% loading with no redundancy and only one redundant SM in each arm, respectively. It can be seen from Fig. 4(a) and (b) that the inclusion of one redundant SM in the MMC with a higher switch rating improves the reliability much more than the case where a switch with a lower rating is used. However, it is essential to remember that the cost of one redundant SM, for example, for a 6.5 kV switch is higher than a 1.2 kV switch. Hence, there is a trade-off between modularity, redundancy, and cost of the MMC. The MMC's B_{10} lifetime without redundancy and one redundant SM in each arm, as shown in Table III, is less than 10 years. In order to reach the required lifetime of 10 years, more redundant SMs are needed. Fig. 4(c) shows the number of redundant SMs required in each arm for the MMC with various switch voltage ratings to meet the 10-year lifetime requirement at 57% loading.

III. CASE-STUDIES FOR COST, RELIABILITY, AND EFFICIENCY-BASED OPTIMAL SWITCH SELECTION

With respect to the total cost of the MMC, the capital investment (CI) and operational losses are considered, which are explained in the following.

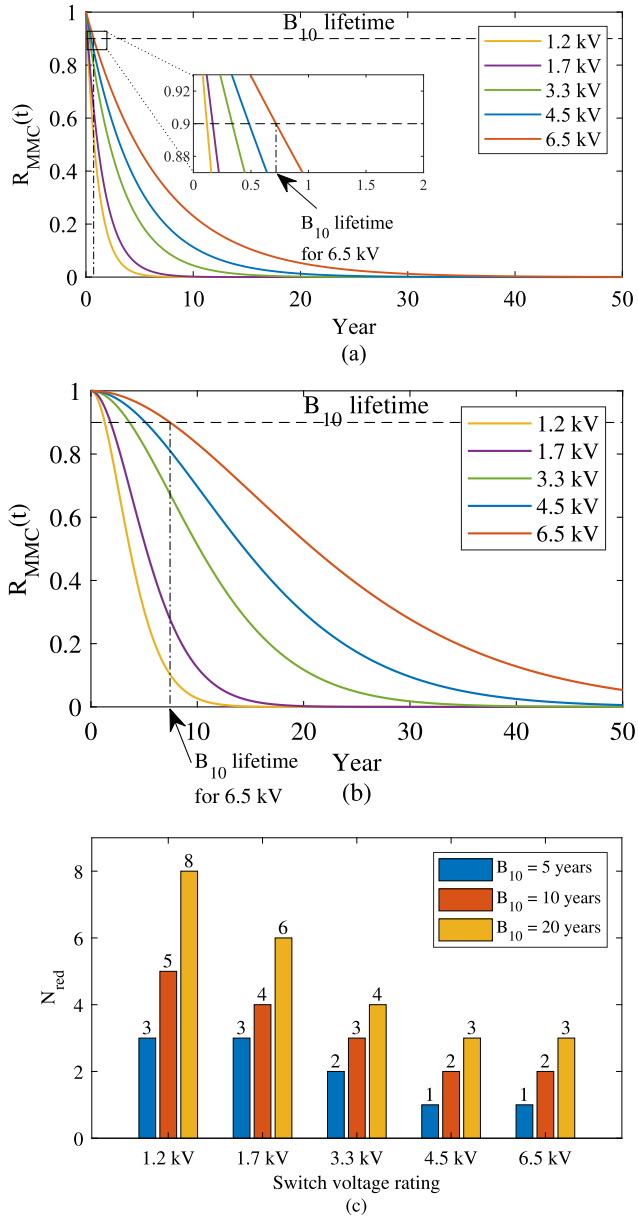

Fig. 4. Reliability results of 10 MW 17 kV DC link MMC with 57% loading, (a) reliability output for different switch voltage rating with no redundancy, (b) reliability output for different switch voltage rating with one redundant SM in each arm, and (c) number of required redundant SM in each arm to meet B_{10} lifetime requirement of 10 years.

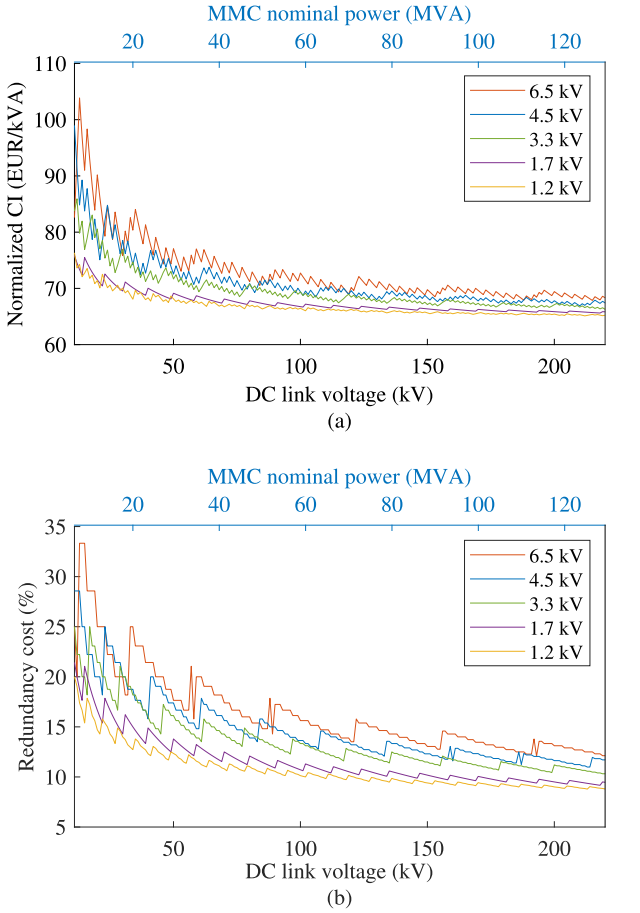

Fig. 5. Cost results of the MMC with 57% loading, (a) normalized CI of the MMC with different switch voltage rating, (b) redundancy percentage of total CI with $B_{10} = 10$ years.

A. Capital Investment

Major components' costs are considered for calculating the CI of the MMC. The dominant components for consideration in CI are power electronics components (semiconductors, control system, power supply) and capacitor cost. Hence, the estimated CI of the power electronics components CI_{PE} is formulated as follows [15]:

$$CI_{\text{PE}} = K_{\text{PE}} N_{\text{semi}} V_{\text{IGBT}} I_{\text{nominal}} \tag{17}$$

where I_{nominal} is the nominal or rated current of the IGBT, which in this study is calculated and equals to 480 A, N_{semi} is the total number of IGBT switches in the MMC that is equal to $N_{\text{semi}} = 6 \times 2 \times n$, K_{PE} is the estimated price of installed power that is equal to € 3.5/kVA [28]. The estimated CI of capacitance (CI_{Cap}) can also be calculated from (18)–(20):

$$CI_{\text{Cap}} = K_{\text{Cap}} E_{\text{Cap}} \tag{18}$$

$$E_{\text{Cap}} = 6 \times n \times E_{\text{Cell}} \tag{19}$$

$$E_{\text{Cell}} = \frac{1}{2} C_{\text{SM}} V_{\text{SM}}^2 \tag{20}$$

where K_{Cap} is the estimated price of the installed capacitor equal to € 150/kJ. Hence, the CI of the MMC can be estimated by adding the CI of installed capacitance and power electronics switches. In Fig. 5(a), the CI of the MMC with different switch ratings for varying DC link voltage at 57% loading is presented. As shown in Fig. 5(a), switch rating of 1.2 kV is the most economical option from the only CI point of view throughout the varying DC link voltage. The normalized price can be obtained from (21).

$$\text{Normalized CI(€/kVA)} = \frac{CI_{\text{total}}}{S_{\text{n}}}, (S_n \text{ in kVA}). \tag{21}$$

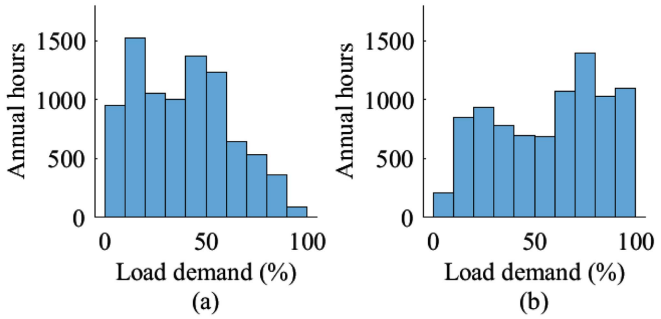

Fig. 6. Histogram of hourly annual power demand for (a) MP I and (b) MP II.

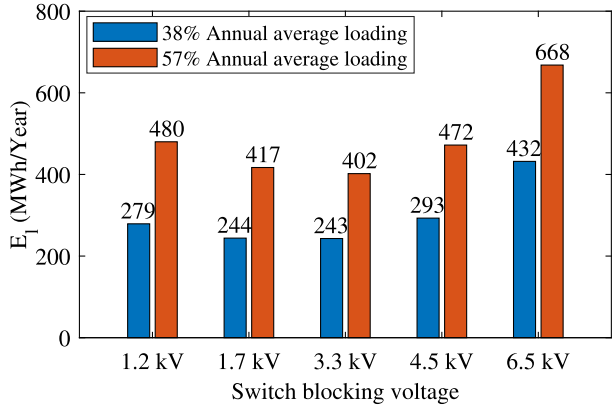

Fig. 7. Cumulative yearly energy losses E_l for 10 MW 17 kV MMC.

As mentioned in section II, redundancy is applied to increase the MMC reliability with various modularity (Fig. 4(b)). However, the cost of using redundancy and CI of the MMC differs for different switch ratings; hence, cost aspects are a determining factor in selecting the cost-efficient switch rating while the reliability requirements are met. Fig. 5(b) presents the ratio of redundancy costs concerning the total CI of the MMC. As shown from Fig. 5(b), applying redundancy has a lower price for higher DC link voltage ranges, while it is more costly for lower DC link voltage ranges. Also, it can be realized that the cost of applying redundancy for the MMC with higher switch voltage rating is more.

B. Operational Losses

The model developed in [29] is applied to obtain the MMC's operational efficiency with various modularity levels. The physics-based methodology explained in [16] is used to estimate the switching and conduction losses of IGBTs. Also, switching and conduction losses are evaluated for varying loading. For calculating the annual energy losses (E_l) with different modularity levels, (22) is applied as follows:

$$E_l = \int (100 - \eta(t_i)) \times P_{\text{MMC}} \tag{22}$$

where $\eta(t_i)$ is the efficiency of the MMC at time t_i and P_{MMC} is the MMC rated power in MW.

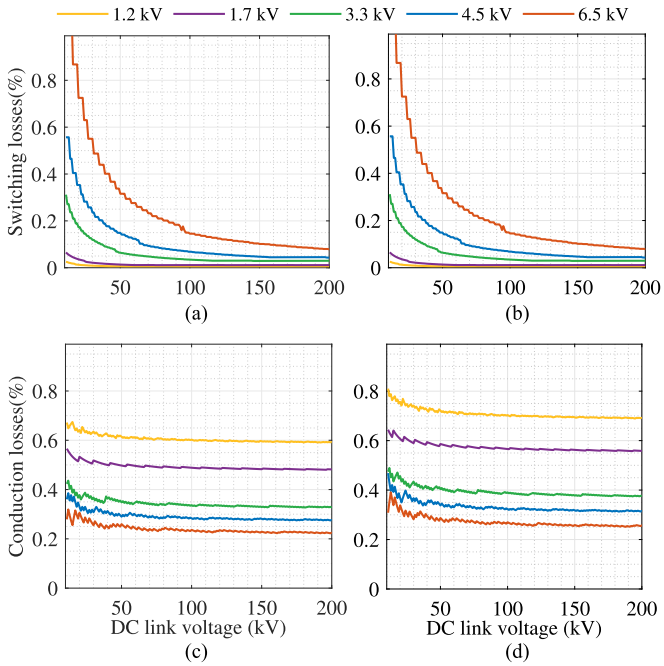

Fig. 8. Losses of the MMC due to (a) switching losses in MP I (b) switching losses in MP II (c) conduction losses in MP I (d) conduction losses in MP II.

C. Case Study for Operational Losses

Fig. 6(a) and (b) show the histogram of two Mission Profiles (MPs) used in this study based on the hourly data adapted from [30]. The average power demand (P_{ave}) of MP I and MP II is 38% and 57%, respectively. Fig. 7 presents the cumulative yearly energy losses for MMC with different switch ratings according to the daily power demand for two cases shown in Fig. 6.

Likewise, these calculations can be repeated for varying DC link voltage other than 17 kV considered. For this evaluation, the phase current is kept constant, and the DC link voltage is changing (as well as the rated power of the MMC). Since the rated current is kept constant, the same switch rating with the same character can be applied, but the number of levels, operational losses, reliability, and CI will change. In Fig. 8, the conduction and switching losses of the MMC are presented. Switching loss is dominant for low DC link voltages, while conduction loss is becoming the dominant factor in higher DC link voltages. Fig. 9 shows the total losses of the MMC for the annual loading shown in Fig. 6 for varying DC link voltage (with 1 kV resolution).

To better clarify the importance of annual loading, two points as P_1 and P_2 are considered from Fig. 9. For MP I, the switch with a rated voltage of 4.5 kV is the most efficient for the DC link voltage range between $P_1 \approx 65$ kV to $P_2 \approx 157$ kV. However, this range is $P_1' \approx 62$ kV to $P_2' \approx 138$ kV when higher average loading corresponding to MP II is considered.

To generalize the scenarios mentioned in this sub-section for two different annual loading, an average annual loading point is considered, which can change from 1% to 100%. Fig. 10 shows

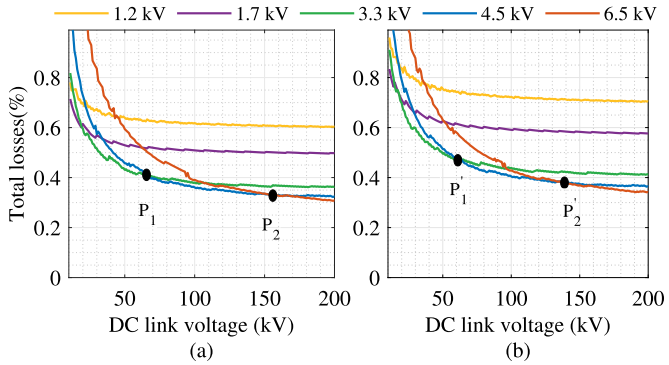

Fig. 9. Total losses of the MMC for varying DC link voltage, (a) MP I and (b) MP II.

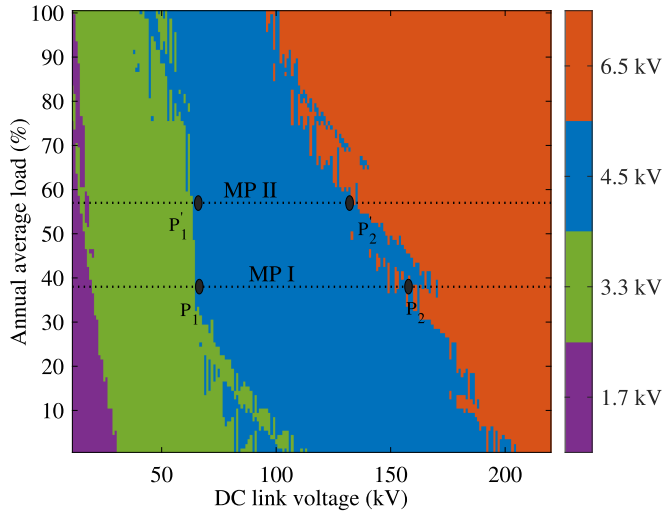

Fig. 10. Optimal switch voltage rating choice map based on the efficiency of the MMC under various annual average loading with varying DC link voltage.

the heat map of the most efficient switch for varying DC link voltage and annual average loading. As it can be seen from Fig. 10, for a DC link voltage higher than 200 kV, switch with 6.5 kV rating voltage is the most efficient choice regardless of the average loading of the converter. For lower DC link voltages, there is a trend between an optimal switch dependent on the MMC's annual average loading. From Fig. 10 can be seen that higher DC link voltage leads to a shift in preference towards higher rated voltage of switch for the same average yearly loading. Likewise, for the same DC link voltage, a higher annual load leads to a shift in preference toward higher switch voltage rating. Please note that the energy savings obtained from constant average annual loading are slightly different when an hourly power demand of MMC is considered. This is shown in Fig. 10 as points P_1, P_2, P_1', and P_2' obtained originally from hourly power demand in Fig. 9. As it can be seen, the points are not exactly on the boundary between switches with 4.5 kV and 6.5 kV ratings, and it is slightly different.

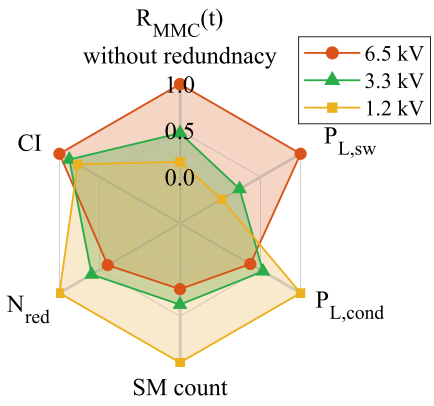

Fig. 11. Overview of the trade-offs for 10 MW 17 kV DC link MMC affected by switch voltage rating.

IV. Sensitivity Analysis for Generalized Switch Voltage Rating Selection

As presented, many variables are needed to determine the most economical switch for every specific DC link voltage and annual average loading. Fig. 11 summarizes the characteristic comparison of the MMC for three switches with rated voltage of 1.2, 3.3, and 6.5 kV. The trend shown in Fig. 11 is valid for all DC link voltages and annual average loading. Nevertheless, combining all these characteristics defines the most economically viable choice for rated voltage of the switch.

A financial index must be defined to compare different rated voltage of switches and find the economic viability range of each switch concerning DC link voltage and annual average loading. This study considers payback as the economic index for determining the most economical switch choice. The payback helps make a financial decision based on how long it takes to get the profit for extra invested money. The CI and savings of the various switch choices are compared to calculate the payback as follows:

$$\text{Payback (PB)} = \frac{\Delta CI}{S_\text{i}} \tag{23}$$

$$S_\text{i} = \int \Delta E_i \times P_\text{t} \tag{24}$$

where ΔCI is the difference of CI between different switch ratings, S_i is the difference in cost saving due to efficiency, ΔE_i (kWh) is the energy saving difference, Pt is the price for electricity that in The Netherlands is equal to 0.190 € /kWh. In this study, the economic viability boundary is defined based on a considered payback time of 10 years. The steps given in the flowchart in Fig. 12 can be followed to find the optimum rated voltage of the switch in the MMC with specified characteristics (DC link voltage and annual load demand). The methodology for finding the cost-efficient switch rating is shown in Fig. 13. This algorithm evaluates if investing extra money in the MMC with the lowest CI to use other switch ratings could have a payback of 10 years or less.

Fig. 14 presents the economic viability regions among various rated voltage of switches for $B_{10} = 10$ years with varying DC

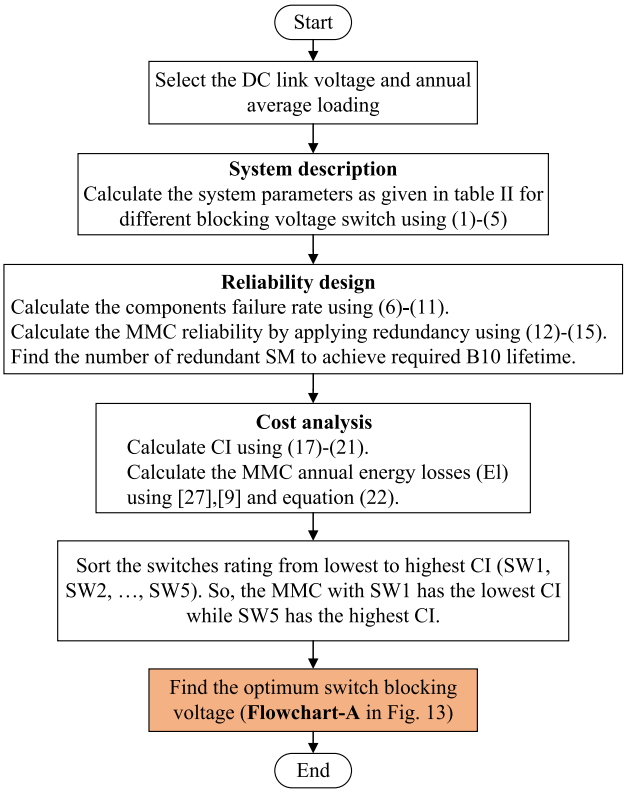

Fig. 12. Flowchart of the proposed methodology for finding the optimum rated voltage of switch.

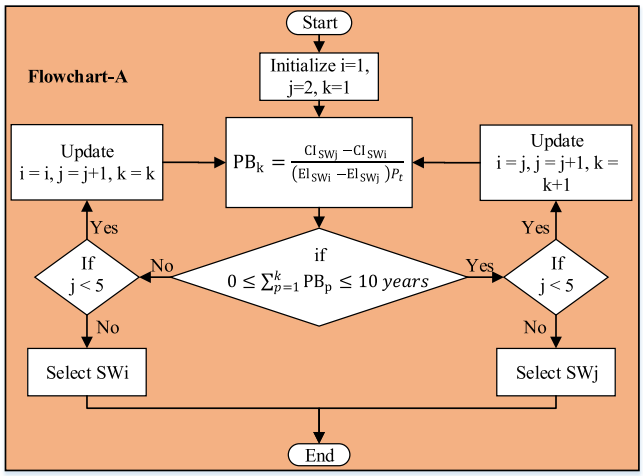

Fig. 13. Algorithm for finding the optimum switch voltage rating among five options.

link voltage and annual average loading considering a 10-year payback. Similar to the obtained heat map of efficiency, the current and voltage rating of the switches are fixed. A comparison is performed among different rated voltage of switches. Fig. 14 suggests that each rated voltage of the switches is more economically viable for a specific DC link voltage and loading. As presented in Fig. 5(a), the MMC with a rating voltage of 1.2 kV has the lowest CI, and Fig. 14 shows if extra money

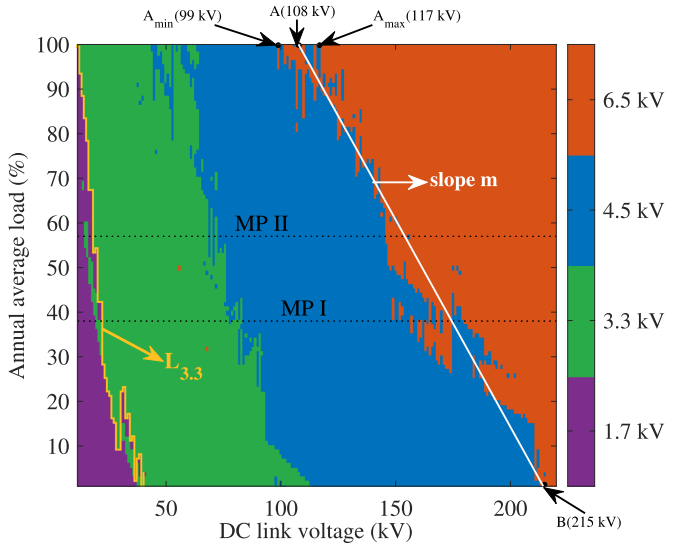

Fig. 14. Economic viability region for different switch voltage rating with variation in MMC loading and DC link voltage considering a payback of 10 years and a required $B_{10} = 10$ years ($L_{3.3}$ is the boundary line between 1.7 kV and 3.3 kV switches).

invested in the MMC with higher switch voltage rating has a payback of 10 years or less. For instance, Fig. 14 suggests that if the DC link voltage is 50 kV and the expected annual loading is 50%, extra investment in the MMC that uses a switch with a rating voltage of 3.3 kV (instead of 1.2 kV and 1.7 kV) will have a payback of 10 years or less.

The two considered case studies are shown with dashed black lines in which fixed load is representative of annual average loading. From Fig. 14 can be seen that in the case of MP II, the switch with a rated voltage of 1.7 kV is the most economical for the range of 10-22 kV DC link voltage. Regarding the case with MP I, 1.7 kV switch is economically viable for DC link voltages between 10 kV and 27 kV. Regarding extra investment in the switch with 3.3 kV rated voltage for MP II, the economically viable DC link voltage is estimated to be between 22 kV and 72 kV. For MP I, the estimated range is 27 kV to 83 kV. The same economically viable DC link range can be estimated for the switches with rated voltage of 4.5 kV and 6.5 kV. Another example is 10 MW 17 kV DC link MMC in which the switch rating of 1.7 kV is the best choice, as shown in Fig. 14. If the lifetime requirement is 10 years, using a switch with a 1.2 kV rating voltage results in lower initial cost (according to Fig. 5). But, choosing a 1.7 kV switch leads to a 15% reduction in operational losses (according to Fig. 9). Hence, in this case, the switch with the rated voltage of 1.7 kV is selected because the extra investment will have a payback of less than 10 years, and it is due to the higher efficiency.

A. *Sensitivity Analysis for Different FR, B_{10} Lifetime Requirement, Components Cost and Energy Price*

The sensitivity of the switch regions' payback to different B_{10} lifetime requirements, FR, component cost, and energy

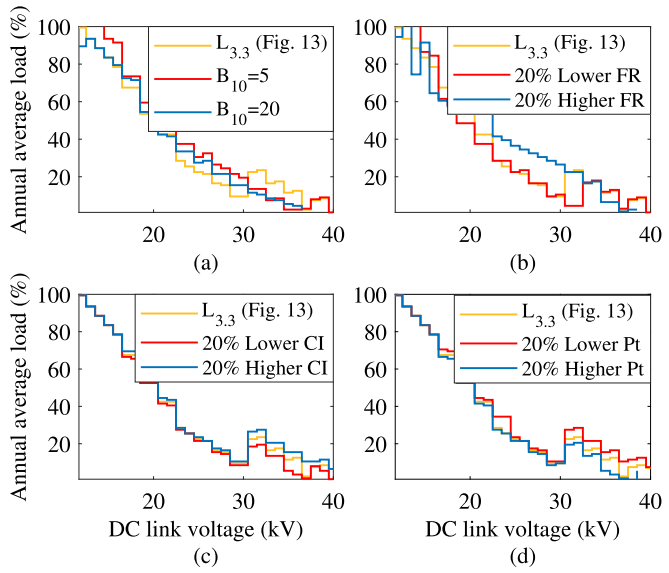

Fig. 15. Shift in $L_{3.3}$ with change in (a) B_{10} lifetime; (b) FR; (c) capital investment (CI), and (d) electricity price (Pt).

price is shown in Fig. 15. The boundary line ($L_{3.3}$) between economic regions of 1.7 kV and 3.3 kV switches is considered since the same trend is valid for other boundary lines between other regions.

The required B_{10} lifetime can vary from 5 to 20 years. hence, the effect of higher or lower required B_{10} lifetime is shown in Fig. 15(a). As can be seen, there is no specific trend with an increase or decrease in the required B_{10} lifetime. As explained in section II B, the methodology in MIL is used to estimate the FR of the IGBT and capacitor. However, the obtained values might not be precise as many environmental factors (π_x) can change the SM's actual FR. Moreover, there are other components within the structure of the SM, such as gate drives, control systems, and power supply, which might experience random failure. Therefore, for sensitivity analysis, the SM's FR's exact value is 20% higher and lower than the obtained values. It can be observed from Fig. 15(b) that the boundary line between regions of 1.7 kV and 3.3 kV switches has a limited dependence on the FR variation.

Considering the component's cost, the dependence of the boundary line on CI is shown in Fig. 15(c). It can be realized that if components are more expensive, the boundary line ($L_{3.3}$) moves upwards quite trivially, and the economic viability region of the switch with 1.7 kV rated voltage (purple) increases. However, an increase in energy price has a reverse effect on the boundary line compared to the CI presented in Fig. 15(d), which is negligible.

B. Sensitivity Analysis by Using MIL and FIDES

In this section, a more recent FIDES method [31] to calculate the FR of components (λ_{FIDES}) is compared with λ_{MIL} used thus far in the paper. Unlike λ_{MIL}, λ_{FIDES} considers the technical control over manufacturing (Π_{pm}), field operation and maintenance (Π_{process}) and physical failure ($\lambda_{\text{physical}}$) that is given by (25) and (26).

TABLE IV
FR OF THE CAPACITOR AND IGBT CONSIDERING MIL AND FIDES

Components	MP	FR (occ/year)	
		FIDES	MIL
IGBT	I	0.00052	0.0017
	II	0.00086	0.0022
Capacitor	I	0.00042	0.0009
	II	0.00068	0.0012

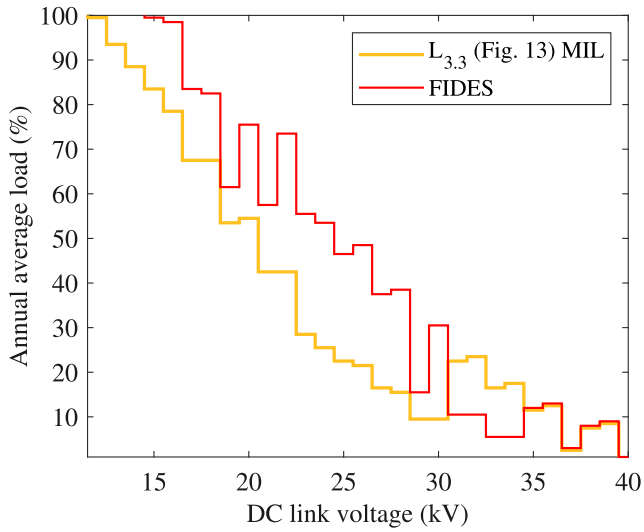

Fig. 16. Shift in $L_{3.3}$ using FIDES and MIL to estimate the component's FR.

$$\lambda_{\text{FIDES}} = \lambda_{\text{physical}} \times \Pi_{\text{pm}} \times \Pi_{\text{process}} \tag{25}$$

$$\lambda_{\text{physical}} = \sum_{i}^{\text{phases}} \left[\frac{t_{\text{annual}}}{8760}\right] \Pi_i \lambda_i \tag{26}$$

where t_{annual} denotes the duration of the i^{th} phase of the mission profile for one year. Π_i and λ_i are associated with environmental and operation stress-specific factors for each phase i. The complete methodology for FIDES is described in [31] and not repeated here for conciseness. Under assumptions corresponding to similar operating and environmental conditions, the estimated λ_{FIDES} compared with λ_{MIL} for the two mission profiles is shown in Table IV.

The sensitivity analysis is carried out to evaluate the impact of FIDES and MIL methods on the boundary line (i.e., $L_{3.3}$ in Fig. 14). Table IV shows that the FIDES method estimates the FR of components to be lower than MIL. Therefore, the shift in the boundary line ($L_{3.3}$) between regions of 1.7 kV and 3.3 kV switches can be seen in Fig. 16. The sensitivity analysis represents that if the FIDES method is used for estimating the FR, the economic viability region of 1.7 kV switch expands for annual average loading of more than 30%.

C. Impact of Converter Power Capacity

The selection of switch voltage rating for various DC link voltage and loading at a fixed rated capacity has been discussed.

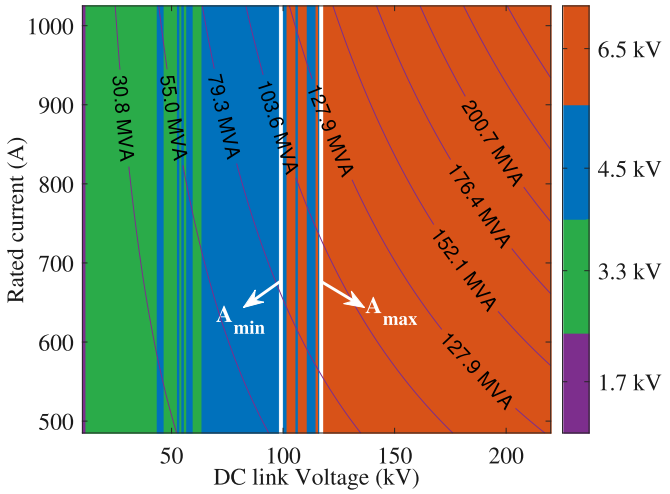

Fig. 17. Economic viability region for different switch voltage rating with variation in MMC current rating and DC link voltage at 100% loading (i.e., 480 A, given in Fig. 14) considering a payback of 10 years and a required $B_{10} = 10$ years.

TABLE V
THE SPECIFICATIONS OF (27)

Transition	$1.7 \leftrightarrow 3.3\,kV$	$3.3 \leftrightarrow 4.5\,kV$	$4.5 \leftrightarrow 6.5\,kV$
m	3.3×10^{-5}	2×10^{-5}	9×10^{-6}
V_{ref}	40 kV	110 kV	220 kV
Voltage range(kV)	$10 \leq V \leq 50$	$50 < V \leq 110$	$110 < V$

In this section, further evaluation is carried out to determine the most economically viable switch rating with variation in current rating and varying DC link voltage at 100% loading. As shown in Fig. 17, the MMC-rated current is changed from 480 A to 1025 A, corresponding to the converter power rating from about 6.5 MVA to 275 MVA. From Fig. 17, it can be observed that the switch rating selection is independent of rated current and only depends on loading and DC link voltage.

V. GENERALIZED APPLICATION SPECIFIC RECOMMENDATIONS

MMC can be applied for different applications having different DC link voltage and current ratings [32]. The most economical switch voltage rating in these applications depends on the selected DC link voltage and loading. In this context, to generalize the proposed method, (27) is derived from Fig. 14.

$$\begin{cases} \text{if } \frac{\text{L}}{100} + \text{m}(V - V_{\text{ref}}) \geq 0, & \text{Select the higher switch rating} \\ \text{else}, & \text{Select the lower switch rating} \end{cases} \tag{27}$$

where L is the annual average loading of the MMC in percentage, m and V_{ref} are specified in Table V, and V is the considered DC link voltage. In Fig. 14, a line with slope m connects two points (A, B) on boundaries between different switch ratings at 100% and 1% loading. For instance, to find these two points between 4.5 kV and 6.5 kV switches at 100% loading, the voltage rating is 108 kV. This voltage rating is calculated by taking the average of A_{min} and A_{max}, as shown in Fig. 14. Thus, points A and B coordinate (108 kV, 100%) and (215 kV, 1%), respectively. Hence, the slope m can be calculated by having these two points.

TABLE VI
OPTIMAL SWITCH VOLTAGE RATINGS FOR DIFFERENT APPLICATIONS

[Ref]	Application	V_{dc}	S_n	P_{Lave}	V_{IGBT} (kV)	
		kV	MVA	%	Used	Optimal
[9]	MVDC Grid	±27	30	60	4.5	3.3
[6]	MVDC Grid	10	3	30	1.7	1.7
[7]	Wind	17	10	10-100 †	4.5	1.7/3.3
[30]	MVDC Grid	17	10	38 & 57	3.3	1.7
[15]	STATCOM	28	17	25-100 †	3.3	1.7/3.3
[17]	HVDC	±320	1000	-	4.5	6.5
[33]	Wind-HVDC	32	18	0-100 †	6.5	1.7/3.3
[34]	Wind-HVDC	160	320	-	3.3	4.5/6.5

† Variable power

For example, in [9], the DC link voltage is 54 kV, and the annual average loading is about 60%. Since the DC link voltage is within the range of the second column of Table V, the second column values are used. After putting these values in (27), it suggests that the most economical rated voltage of the switch is 3.3 kV. However, 4.5 kV switch is used in [9], which is overrated and can impact the cost and efficiency of the system. Table VI summarizes some of the MMC applications found in the literature and shows the optimal rated voltage of the switch using the proposed method.

VI. CONCLUSION

This article presents cost-oriented reliability and modularity-based trade-offs to select an optimal rated voltage of the switch for MMC. The steps involved in the proposed method are explained through flowcharts, and a heat map is provided for varying DC link voltage and yearly loading of the MMC. It is presented that the system's modularity increases when a lower switch voltage rating is selected for the MMC SMs. For example, in a 10 MW MMC with a DC link voltage of 17 kV, a switch rating of 1.7 kV is optimal for both case studies. Higher modularity can be achieved with 1.2 kV rated voltage with a lower CI for a B_{10} lifetime of 10 years. But, when 1.7 kV switch is selected instead of 1.2 kV switch, the operational losses are approximately 15% lower in both cases (MP I and MP II), leading to payback of less than 10 years. Higher DC link voltage leads to a shift in preference towards a higher switch rating for the same average loading. For example, the optimal choice of switch rated voltage changes from 1.7 kV to 3.3 kV in both case studies (MP I and MP II) if the given DC link voltage is increased from 17 kV to 50 kV. Transitions between preferred switch ratings with variation in DC voltages between 10-220 kV are shown for different average loading. The sensitivity analysis shows that the preference's boundary changes from 1.7 kV to 3.3 kV switch rating shifts downward slightly with lower CI and higher energy price. However, the preferred switch choices show limited sensitivity to variation in required B_{10} lifetime and assumed FR of individual components. Also, the preference's boundary from 1.7 kV to 3.3 kV shifts downward if FIDES methodology is used for estimating the components FR.

In conclusion, this study proposed selection regions for the optimum rated voltage of the switch in the MMC for varying

DC link voltage and yearly load demand. Sensitivity analysis shows that for MMC with fixed-level active redundancy, the variation among switches' regions has limited dependence on the precise FR value and required B_{10} lifetime. Also, it was observed that changes in CI and energy prices have a negligible effect. However, using the methodology proposed in FIDES for calculating the FR can affect the region as a specific trend was realized for annual loading higher than 30%. The effectiveness of the method proposed in this study is demonstrated by presenting a generalized version of it and applying it in published works.

REFERENCES

[1] J. Jia, G. Yang, and A. H. Nielsen, "A review on grid-connected converter control for short-circuit power provision under grid unbalanced faults," *IEEE Trans. Power Del.*, vol. 33, no. 2, pp. 649–661, Apr. 2018.

[2] R. Abe, H. Taoka, and D. McQuilkin, "Digital grid: Communicative electrical grids of the future," *IEEE Trans. Smart Grid*, vol. 2, no. 2, pp. 399–410, Jun. 2011.

[3] S. Du, B. Wu, and N. Zargari, "Common-mode voltage minimization for grid-tied modular multilevel converter," *IEEE Trans. Ind. Electron.*, vol. 66, no. 10, pp. 7480–7487, Oct. 2019.

[4] S. Yang, A. T. Bryant, P. Mawby, D. Xiang, L. Ran, and P. J. Tavner, "An industry-based survey of reliability in power electronic converters," *IEEE Trans. Ind. Appl.*, vol. 47, no. 3, pp. 1441–1451, May/Jun. 2011.

[5] V. D. N. Ferreira et al., "Design and selection of high reliability converters for mission critical industrial applications: A rolling mill case study," *IEEE Trans. Ind. Appl.*, vol. 54, no. 5, pp. 4938–4947, Sep./Oct. 2018.

[6] P. Tu, S. Yang, and P. Wang, "Reliability- and cost-based redundancy design for modular multilevel converter," *IEEE Trans. Ind. Electron.*, vol. 66, no. 3, pp. 2333–2342, Mar. 2019.

[7] H. Li et al., "Cost and reliability optimization of modular multilevel converter with hybrid submodule for offshore DC wind turbine," *Int. J. Elect. Power Energy Syst.*, vol. 120, 2020, Art. no. 105994.

[8] B. Wang, X. Wang, Z. Bie, P. D. Judge, X. Wang, and T. C. Green, "Reliability model of MMC considering periodic preventive maintenance," *IEEE Trans. Power Del.*, vol. 32, no. 3, pp. 1535–1544, Jun. 2017.

[9] G. Abeynayake, G. Li, T. Joseph, J. Liang, and W. Ming, "Reliability and cost-oriented analysis, comparison and selection of multi-level MVdc converters," *IEEE Trans. Power Del.*, vol. 36, no. 6, pp. 3945–3955, Dec. 2021.

[10] X. Xie et al., "Reliability modeling and analysis of hybrid MMCs under different redundancy schemes," *IEEE Trans. Power Del.*, vol. 36, no. 3, pp. 1390–1400, Jun. 2021.

[11] J. Guo, X. Wang, J. Liang, H. Pang, and J. Gonçalves, "Reliability modeling and evaluation of MMCs under different redundancy schemes," *IEEE Trans. Power Del.*, vol. 33, no. 5, pp. 2087–2096, Oct. 2018.

[12] J. Xu, H. Jing, and C. Zhao, "Reliability modeling of MMCs considering correlations of the requisite and redundant submodules," *IEEE Trans. Power Del.*, vol. 33, no. 3, pp. 1213–1222, Jun. 2018.

[13] J. Xu, P. Zhao, and C. Zhao, "Reliability analysis and redundancy configuration of MMC with hybrid submodule topologies," *IEEE Trans. Power Electron.*, vol. 31, no. 4, pp. 2720–2729, Apr. 2016.

[14] J. Xu, L. Wang, D. Wu, H. Jing, and C. Zhao, "Reliability modeling and redundancy design of hybrid MMC considering decoupled sub-module correlation," *Int. J. Elect. Power Energy Syst.*, vol. 105, pp. 690–698, 2019.

[15] J. V. M. Farias, A. F. Cupertino, V. d. N. Ferreira, H. A. Pereira, S. I. Seleme, and R. Teodorescu, "Reliability-oriented design of modular multilevel converters for medium-voltage STATCOM," *IEEE Trans. Ind. Electron.*, vol. 67, no. 8, pp. 6206–6214, Aug. 2020.

[16] J. E. Huber and J. W. Kolar, "Optimum number of cascaded cells for high-power medium-voltage AC–DC converters," *IEEE Trans. Emerg. Sel. Topics Power Electron.*, vol. 5, no. 1, pp. 213–232, Mar. 2017.

[17] J. Guo, J. Liang, X. Zhang, P. D. Judge, X. Wang, and T. C. Green, "Reliability analysis of MMCs considering submodule designs with individual or series-operated IGBTs," *IEEE Trans. Power Del.*, vol. 32, no. 2, pp. 666–677, Apr. 2017.

[18] R. Alvarez, M. Wahle, H. Gambach, and J. Dorn, "Optimum semiconductor voltage level for MMC submodules in HVDC applications," in *Proc. 18th Eur. Conf. Power Electron. Appl.*, 2016, pp. 1–9.

[19] K. Ilves, S. Norrga, L. Harnefors, and H.-P. Nee, "On energy storage requirements in modular multilevel converters," *IEEE Trans. Power Electron.*, vol. 29, no. 1, pp. 77–88, Jan. 2014.

[20] J. V. M. Farias, A. F. Cupertino, H. A. Pereira, S. I. S. Junior, and R. Teodorescu, "On the redundancy strategies of modular multilevel converters," *IEEE Trans. Power Del.*, vol. 33, no. 2, pp. 851–860, Apr. 2018.

[21] A. Shekhar, L. B. Larumbe, T. B. Soeiro, Y. Wu, and P. Bauer, "Number of levels, arm inductance and modulation trade-offs for high power medium voltage grid-connected modular multilevel converters," in *Proc. 10th Int. Conf. Power Electron. ECCE Asia*, 2019, pp. 1–8.

[22] J. He, Q. Yang, and Z. Wang, "On-line fault diagnosis and fault-tolerant operation of modular multilevel converters – A comprehensive review," *CES Trans. Elect. Mach. Syst.*, vol. 4, no. 4, pp. 360–372, 2020.

[23] MIL-HDBK-217F Military Handbook for Reliability Prediction of Electronic Equipment, Washington, DC, USA: Department of Defense, 1990.

[24] K. Hu, Z. Liu, Y. Yang, F. Iannuzzo, and F. Blaabjerg, "Ensuring a reliable operation of two-level IGBT-based power converters: A review of monitoring and fault-tolerant approaches," *IEEE Access*, vol. 8, pp. 89988–90022, 2020.

[25] R. Billinton and R. N. Allan, "Reliability evaluation of engineering systems: Concepts and techniques," USA: Springer, 1992, pp. 1–453.

[26] J. Falck, C. Felgemacher, A. Rojko, M. Liserre, and P. Zacharias, "Reliability of power electronic systems: An industry perspective," *IEEE Ind. Electron. Mag.*, vol. 12, no. 2, pp. 24–35, Jun. 2018.

[27] Y. Zhang, H. Wang, Z. Wang, Y. Yang, and F. Blaabjerg, "Impact of lifetime model selections on the reliability prediction of IGBT modules in modular multilevel converters," in *Proc. IEEE Energy Convers. Congr. Expo.*, 2017, pp. 4202–4207.

[28] H. A. B. Siddique, A. R. Lakshminarasimhan, C. I. Odeh, and R. W. D. Doncker, "Comparison of modular multilevel and neutral-point-clamped converters for medium-voltage grid-connected applications," in *Proc. IEEE Int. Conf. Renewable Energy Res. Appl.*, 2016, pp. 297–304.

[29] A. Shekhar, T. B. Soeiro, Z. Qin, L. Ramírez-Elizondo, and P. Bauer, "Suitable submodule switch rating for medium voltage modular multilevel converter design," in *Proc. IEEE Energy Convers. Congr. Expo.*, 2018, pp. 3980–3987.

[30] A. Shekhar, T. B. Soeiro, L. Ramírez-Elizondo, and P. Bauer, "Offline reconfigurability based substation converter sizing for hybrid AC–DC distribution links," *IEEE Trans. Power Del.*, vol. 35, no. 5, pp. 2342–2352, Oct. 2020.

[31] "FIDES guide 2009 edition: A reliability methodology for electronic systems," 2010. [Online]. Available: www.fides-reliability.org

[32] M. Priya, P. Pathipooranam, and M. Kola, "Modular multilevel converter topologies and applications—A review," *IET Power Electron.*, vol. 12, no. 2, pp. 170–183, 2019.

[33] H. Liu, K. Ma, Z. Qin, P. C. Loh, and F. Blaabjerg, "Lifetime estimation of MMC for offshore wind power HVDC application," *IEEE Trans. Emerg. Sel. Topics Power Electron.*, vol. 4, no. 2, pp. 504–511, Jun. 2016.

[34] G. Guo et al., "HB and FB MMC based onshore converter in series-connected offshore wind farm," *IEEE Trans. Power Electron.*, vol. 35, no. 3, pp. 2646–2658, Mar. 2020.

Miad Ahmadi (Graduate Student Member, IEEE) received the B.Sc. degree in electrical engineering from Razi University, Kermanshah, Iran, in 2016, and the M.Sc. degree in electrical engineering from Politecnico di Milano, Milan, Italy, in 2019. He is currently working toward the Ph.D. degree with DC Systems, Energy Conversion and Storage Group, Delft University of Technology, Delft, The Netherlands. In 2019, he was an R&D Intern with Supergrid Institute, Villeurbanne, France, where he evaluated the reliability of the bus-bar system in high voltage systems. His research interest includes the reliability of power systems, the reliability of power electronics, and the integration of renewable energy sources.

Aditya Shekhar (Member, IEEE) received the bachelor's degree (Hons.) in electrical from the National Institute of Technology, Surat, India, in 2010, and the M.Sc. (*cum laude*) and Ph.D. degrees in electrical engineering from the Delft University of Technology, Delft, The Netherlands, in June 2015 and January 2020, respectively. He is currently an Assistant Professor with the DC systems, Energy Conversion and Storage Group, Department of Electrical Sustainable Energy, Delft University of Technology.

Pavol Bauer (Senior Member, IEEE) received the master's degree in electrical engineering from the Technical University of Kosice, Kosice, Slovakia, in 1985, and the Ph.D. degree from the Delft University of Technology, Delft, The Netherlands, in 1995. From 2002 to 2003, he was with KEMA (DNV GL), Arnhem, The Netherlands, on different projects related to power electronics applications in power systems. He is currently a Full Professor with the Department of Electrical Sustainable Energy, Delft University of Technology, and the Head of DC Systems, Energy Conversion, and Storage Group. He is also a Professor with the Brno University of Technology, Brno, Czech Republic, and an Honorary Professor with the Politehnica University Timişoara, Timişoara, Romania. He has authored or coauthored more than 120 journal articles and 500 conference papers in his field. He is an author or coauthor of eight books, holds seven international patents, and organized several tutorials at international conferences. He has worked on many projects for the industry concerning wind and wave energy, power electronic applications for power systems such as smarttrafo, HVDC systems, projects for smart cities such as photovoltaic (PV) charging of electric vehicles, PV and storage integration, contactless charging; and he participated in several Leonardo da Vinci and H2020, and Electric Mobility Europe EU projects as a Project Partner (ELINA, INETELE, E-Pragmatic, Micact, Trolley 2.0, OSCD, P2P, and Progressus) and a Coordinator (PEMCWebLab.com-Edipe, SustEner, Eranet DCMICRO). Prof. Bauer is the Former Chairman of Benelux IEEE Joint Industry Applications Society, Power Electronics and Power Engineering Society Chapter, the Chairman of the Power Electronics and Motion Control Council, a Member of the Executive Committee of European Power Electronics Association, and also a Member of the International Steering Committee at numerous conferences.